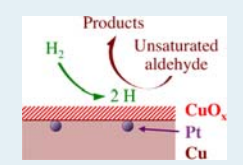


Controlling Selectivity in Unsaturated Aldehyde Hydrogenation Using Single-Site Alloy Catalysts

Yueqiang Cao,^{†,‡} Bo Chen,[†] Jonathan Guerrero-Sánchez,[§] Ilkeun Lee,[†] Xinggui Zhou,[‡] Noboru Takeuchi,^{†,§} and Francisco Zaera*,[†]

Supporting Information

ABSTRACT: Selectivity in catalysis is key to many industrial processes, yet it is often difficult to control. One promising approach is to use so-called single-atom catalysts, whereby one catalytic component is isolated within a second phase to add a key but otherwise unavailable functionality. Here, we report the use of metal alloys consisting of Pt single atoms diluted within Cu nanoparticles to selectively promote the hydrogenation of C=O bonds in unsaturated aldehydes, a reaction of interest in fine chemical manufacturing. Our rationale, that Cu surfaces may favor C=O over C=C hydrogenation



steps with atomic hydrogen but may require Pt sites to promote the initial activation of molecular hydrogen, was corroborated by kinetic catalytic experiments. However, fundamental surface science studies and quantum mechanics calculations showed that the explanation for the observed catalytic performance is more nuanced. For one, titration experiments using carbon monoxide failed to identify Pt atoms accessible on the surface of the catalysts, suggesting that their catalytic contribution may involve indirect electronic changes on neighboring Cu atoms. In addition, infrared absorption and X-ray photoelectron spectroscopy results identified the existence of a thin Cu oxide layer covering the metallic nanoparticles. Finally, it was determined that hydrogenation selectivity with Cu-based catalysts may be explained in part by their preference for bonding unsaturated aldehydes via the terminal oxygen atom but is also affected by competitive adsorption among the reactants and products. Single-atom alloy catalysts appear to indeed help with selectivity in hydrogenation catalysis, but more in situ (or operando) characterization experiments are needed to better understand how they operate.

KEYWORDS: selective hydrogenation, unsaturated aldehydes, alloy catalysts, platinum, copper, infrared absorption spectroscopy, DFT, surface chemistry

1. INTRODUCTION

Heterogeneous catalysis is used extensively in industry as a way to accelerate chemical conversions. Most early applications involved relatively simple reactions, but many complex chemical systems have been addressed in recent years using catalysis as well, in petrochemistry and in the manufacturing of fine and speciality chemicals, for instance. In these cases, selectivity takes center stage, as selective processes minimize the consumption of feedstocks, avoid undesirable separation steps, and produce less potentially polluting by-products.²⁻⁴ However, controlling selectivity in catalysis can be quite difficult, especially in hydrogenation reactions with organic feedstocks. One problem that continues to challenge chemists is the promotion of the hydrogenation of C=O bonds in the presence of C=C bonds in organic reactants such as unsaturated aldehydes.^{6–9} Many approaches have been tested to address this issue, where selectivity needs to be controlled directly by tuning the relative rates of two parallel hydrogenation steps, but perhaps the most promising has proven to be the use of multimetallic catalysts. 5,10 Platinum-based catalysts are quite good at promoting hydrogenations in

general but tend to display poor selectivity; so, the addition of a second element has been attempted as a way to provide further control over such selectivity. Conversely, other metals may be chosen first to tune selectivity, and these may be then modified with the added elements to improve activity. The latter is the approach taken here.

Below, we summarize what we have learned about the performance of so-called single-site alloy catalysts, where minor amounts of a second metal (Pt in our case) are added to the first (Cu), for the selective hydrogenation of unsaturated aldehydes. We show that these alloyed catalysts are indeed quite selective toward the hydrogenation of C=O bonds, in particular those with very small amounts of Pt added. We also provide evidence from surface science experiments and density functional theory (DFT) calculations to argue that the main hydrogenation steps take place on the Cu surface. On the other hand, no surface Pt could be detected via titration experiments

Received: June 17, 2019 Revised: August 28, 2019



[†]Department of Chemistry and UCR Center for Catalysis, University of California, Riverside, California 92521, United States [‡]State Key Laboratory of Chemical Engineering, East China University of Science and Technology, 130 Meilong Road, Shanghai 200237, China

[§]Centro de Nanociencias y Nanotecnología, Universidad Nacional Autónoma de México, Apartado Postal 14, Ensenada, Baja California 22800, Mexico

using infrared absorption spectroscopy and carbon monoxide as a probe molecule. X-ray photoelectron spectroscopy (XPS) data indicated that the surface of the catalysts is covered with a thin CuO_x layer instead. These latter observations question the simple interpretation where Pt atoms are located individually on the surface and promote H_2 activation individually, and suggest a more complex cooperative effect instead.

2. EXPERIMENTAL AND COMPUTATIONAL DETAILS

All catalysts were prepared by using an incipient wetness impregnation method. Appropriate amounts of copper nitrate (Cu(NO₃)₂·3H₂O, Sigma-Aldrich, 98% purity) and chloroplatinic acid (H₂PtCl₄·6H₂O, Sigma-Aldrich, \geq 37.50% Pt basis) were mixed with deionized water, and approximately 2 g of commercial SBA-15 (ACS Material) was then impregnated with the liquid solution. The nominal loading of Cu was 5 wt % in all cases, and the Pt/Cu molar ratio was tuned by changing the amount of added chloroplatinic acid. The impregnated samples were kept at room temperature for 24 h, dried at about 350 K for 24 h, and grounded to powder form. All catalysts were reduced at 625 K under H₂ for 3 h prior to their use.

For the kinetic measurements of the catalytic reaction, approximately 0.1 g of the catalyst was added to the reactor vessel (a 300 mL high-pressure 4560 bench Parr batch reactor) previously filled with 75 mL of isopropanol (Sigma-Aldrich, ≥99.7% purity, used as the solvent), 0.8 g of cinnamaldehyde (CMA, Sigma-Aldrich, ≥95% purity), and 2 mL of benzyl alcohol (Sigma-Aldrich, 99.8% purity, used as an internal standard). The vessel was purged five times with 10 bar of H₂ (Liquid Carbonic, >99.995% purity) and then pressurized to the reaction H₂ pressure. After heating to the reaction temperature (375 K), stirring was switched on, and the time was set to zero. Aliquots (1 mL) were taken at preset times and analyzed using an Agilent 6890N gas chromatograph with an HP-50 column (15 m \times 320 μ m \times 0.25 μ m) to determine their composition. Turnover frequencies (TOFs, Supporting Information Figure S2) were estimated in terms of molecules converted per surface metal atom (Cu or Pt) by using the nanoparticle (NP) size distributions from transmission electron microscopy (TEM) characterization of the catalysts, assuming spherical shapes and bulk metal densities.

The transmission Fourier transform infrared (FTIR) spectroscopy characterization experiments were performed on a Bruker Tensor 27 FTIR spectrometer equipped with a deuterated triglycine sulfate (DTGS) detector. About 15 mg of the catalyst was pressed into a self-supporting wafer and loaded inside a homemade quartz cell with NaCl windows.1 The catalyst wafer was reduced in situ at 625 K under 200 Torr H₂ for 3 h, after which the cell was evacuated and cooled down, to room temperature for the experiments with crotonaldehyde (CTA, Sigma-Aldrich, ≥99% purity), and to 123 K (using liquid nitrogen) for CO (Matheson Tri-Gas, ≥99.5% purity) adsorption studies. Afterward, the sample was exposed to either 5 Torr of CTA or 50 Torr of CO for 0.5 h (respectively), and the cell was evacuated for 10 min. With CO, IR spectra were recorded from 125 to 475 K, at 20 K intervals, as the sample and cell were warmed up, and corrected using background spectra obtained under the same condition before adsorption. In the case of the aldehyde, spectra were taken only at 300 and 445 K. All spectra were acquired with a resolution of 2 cm⁻¹, and correspond to an average of 16 scans (chosen so that the spectra could be

acquired in 20 K intervals during the heating of the sample, as mentioned above).

The scanning TEM (STEM) images were acquired using a FEI Titan Themis 300 instrument equipped with a super-X energy-dispersive X-ray spectrometer system. The ex situ XPS analysis was carried out using a Kratos analytical AXIS instrument equipped with a 165 mm mean radius semihemispherical electron energy analyzer and a monochromatized Al anode X-ray source. The Cu 3p peaks were deconvoluted using Gaussian functions once a Shirley background was subtracted to identify the individual contributions from metallic and oxidized Cu.

The regular and isothermal temperature-programmed desorption (TPD and IsoTPD, respectively) experiments were performed in an ultrahigh vacuum (UHV) apparatus equipped with a UTI quadrupole mass spectrometer as well as with XPS instrumentation (to determine the cleanliness of the surfaces).¹³ A Cu single-crystal disk, cut to expose its (110) facet, was mounted on a manipulator capable of liquid nitrogen cooling and resistive heating and cleaned in situ before each experiment via sputtering-annealing cycles followed by annealing until the surface was deemed clean by XPS and CO TPD. For the experiments on oxidized samples, the surface was exposed to 50 L (1 L = 1 \times 10⁻⁶ Torr s) of O₂ at 500 K, and for the regular TPD experiments, the surface was then saturated with atomic hydrogen, produced by flowing H₂ (3 × 10^{-6} Torr \times 300 s) through a hot W filament placed in front of the Cu(110) crystal, about 5 cm away. CMA was dosed afterward, 5000 L at 300 K to ensure monolayer saturation, and the temperature ramped at a linear rate of 4 K/s. In the case of the IsoTPD experiments, the CMA-dosed Cu surface was first heated to the reaction temperature, 325 K, and then the W filament was turned on and the reaction was initiated by opening the leak valve used to introduce the H_2 gas ($P = 3 \times$ 10⁻⁶ Torr). Up to 15 different masses were monitored in each single TPD run in both TPD and IsoTPD experiments by using a personal computer interfaced to the mass spectrometer.

The quantum mechanics calculations were carried out using periodic DFT, similar to what has been reported in a previous work from our group. 14 The Vienna Ab initio Simulation Package¹⁵ was used, with projector-augmented waves. 16 The exchange-correlation energy was modeled with the generalized gradient approximation as stated in the Perdew-Burke-Ernzerhof parameterization. 17 van der Waals interactions were included with empirical dispersion corrections (DFT-D3).18 The electronic states were expanded in plane waves with an energy cutoff of 400 eV. Either (3×3) or (2×2) surface unit cells were used to emulate adsorbate coverages of 0.11 and 0.25 ML, respectively; they were 4 atomic layers in thickness, with a 15 Å vacuum space added in the z direction. The Brillouin zone integration was done using k-point grids of $3 \times 3 \times 1$ and $5 \times 5 \times 1$ for the (3×3) and (2×3) \times 2) surface periodicities, respectively.

3. RESULTS AND DISCUSSION

We started our search for a more selective hydrogenation catalyst with Cu-based catalysts, as some past reports had suggested that Cu may be a viable choice to preferentially promote C=O over C=C bond hydrogenation¹⁹ (although the existing literature is not conclusive on this point).²⁰ The main problem with Cu, however, is that it is quite inefficient at activating molecular hydrogen.²¹ To overcome this limitation, we added isolated Pt atoms to the Cu NPs, following the

single-atom catalysis approach being promoted by many researchers. $^{22-25}$ Specifically, we build on the detailed study of Cu–Pt catalysts reported by the groups of Sykes and Flytzani-Stephanopoulos, $^{26-29}$ which includes the successful test of other hydrogenation reactions. Their model proposes that the role of the Pt atoms is to dissociate H_2 , after which the resulting adsorbed H atoms spill over to the Cu surface and react with the adsorbed hydrocarbons.

In this study, a family of $\text{CuPt}_x/\text{SBA-15}$ catalysts with Pt content as low as 0.1 mol % (x=0.001) was prepared via coimpregnation on a mesoporous silica-based support (SBA-15) to be used for the hydrogenation of CMA (3-phenyl-prop-2-enal) to cinnamyl alcohol (3-phenyl-prop-2-enol, CMO) selectively over the competing production of dihydrocinnamaldehyde (3-phenyl-propanal, HCMA) or the fully hydrogenated dihydrocinnamyl alcohol (3-phenyl-propanol, HCMO). As hypothesized, it was found that the $\text{CuPt}_x/\text{SBA-15}$ catalysts improve selectivity in the conversion of CMA to CMO when compared to the performance of single-metal Pt or Cu catalysts. Data from our kinetic studies, exemplified by the results reported in Figure 1, show that the total conversion

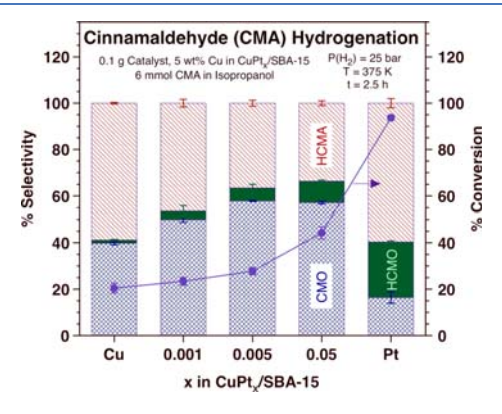


Figure 1. Total conversion after 2.5 h of reaction (purple filled circles and right-hand side scale) and selectivities (bars, left axis) for the hydrogenation of CMA using Cu–Pt bimetallic catalysts dispersed on SBA-15 (CuPt_x/SBA-15) as a function of their metal composition. Optimum selectivity for the hydrogenation of the C=O bond in CMA to produce CMO (blue cross-hatched bars), which competes with the parallel C=C hydrogenation step to HCMA (striped red bars) and with total hydrogenation to HCMO (green solid bars), is obtained with alloys made out of very diluted amounts of Pt in Cu, for a CuPt_{0.005}/SBA-15 composition in this example.

(purple filled circles, right scale) is significantly higher with pure Pt catalysts than with any of the Cu-containing samples but that selectivity toward the production of CMO, the desired product, is higher with Cu. Furthermore, the addition of small amounts of Pt to the Cu catalyst leads to significant further improvements in both activity (compared to the pure Cu catalyst) and selectivity (compared to both pure Cu and pure Pt catalysts). Under the conditions of the experiments reported in Figure 1, the optimum in CMO selectivity (blue crosspatterned bars) was seen with the CuPt_{0.005}/SBA-15 catalyst, which corresponds to a 0.5 mol % Pt content. An interesting observation associated with these trends is the fact that the improved selectivity is mainly associated with a lower activity for CMA hydrogenation to HCMA on the Cu-based catalysts, which becomes even lower when small amounts of Pt are added; the absolute CMO production rate is affected to a much lesser extent by the composition of the bimetallic NPs.

The pure Pt catalyst is also much more active toward the full hydrogenation reaction to HCMO. Similar trends were observed at different hydrogen pressures (Supporting Information Figure S1) and also when following TOFs as a function of reaction time (Supporting Information Figure S2).

To better understand the molecular basis for this improved catalytic behavior, a series of fundamental experimental studies and quantum mechanics calculations were performed. Our general conclusion is that the explanation for why the CuPt_x-based samples display such a unique catalytic behavior is more nuanced than that implied by the simplistic single-atom alloy catalysis model.

We start by discussing the role of Pt. Electron microscopy was used to assure that, indeed, the catalysts made here consist of true bimetallic NPs dispersed on the oxide support (Figure 2). This is the most evident in the energy-dispersive X-ray

CuPt_{0.75}/SBA-15 TEM & EDS

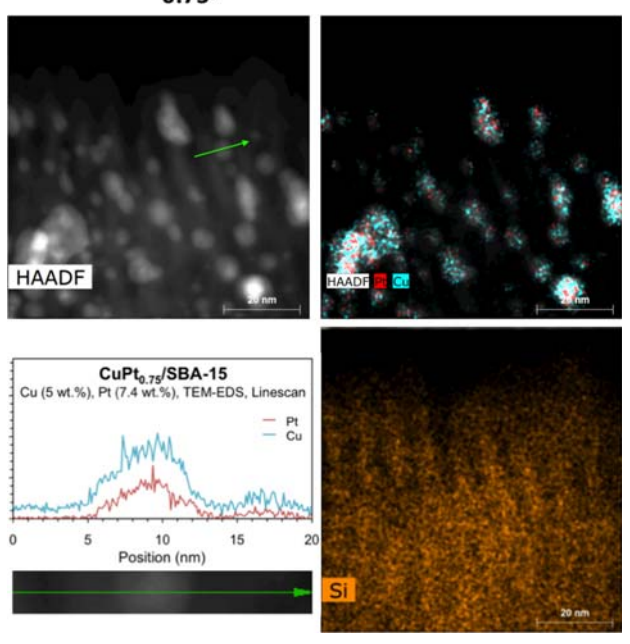


Figure 2. Electron microscopy characterization of our $\text{CuPt}_{0.75}/\text{SBA-15}$ catalyst. Upper left: High-angle annular dark-field (HAADF) STEM image. Upper right: EDS image, with the Pt and Cu atoms colored in red and blue, respectively. Lower left: EDS composition scan across an individual metal NP, indicated by the green arrow in the panel above. Lower right: EDS image of the Si atoms, highlighting the orientation of the pores in the SBA-15 support. These images indicate that the bimetallic NPs are located inside the mesopores of the SBA-15 support and that the Pt is dissolved and dispersed in atomic form within the Cu NPs. The scaling bars provided in the lower right corner of the three images correspond to 20 nm.

spectroscopy (EDS) image shown in the upper right panel of Figure 2, which clearly shows not only that the Pt atoms (red) are located within the Cu NPs (blue) but also that they are well dispersed in individual atomic forms, even in catalysts with a relatively high Pt content (x = 0.75 in this example).

Next, we explore the placement of the Pt atoms in terms of the surface versus the bulk of the bimetallic NPs in the CuPt_x/SBA-15 catalysts. The XPS data reported in Figure 3 indicate that some Pt atoms are detectable in the near surface, within the detection depth of the technique (a couple of nanometers):

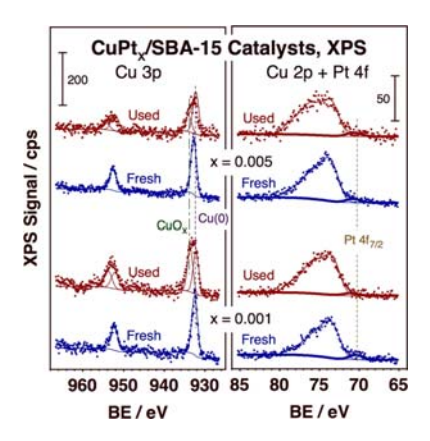


Figure 3. Cu 3p (left panel) and Cu 2p + Pt 4f (right) XPS from the CuPt_{0.001}/SBA-15 (bottom two traces) and CuPt_{0.005}/SBA-15 (top two traces) catalysts before ("fresh", blue traces) and after ("used", red traces) their use to promote the hydrogenation of CMA. The experimental data are shown as dots, whereas the solid lines in the Cu 3p data are fits to Gaussian peaks after adjusting for the (Shirley) background signal. A small Pt $4f_{7/2}$ peak is clearly seen at a BE of 70.7 \pm 0.3 eV in the right panel in spite of the low concentration of that metal in the bimetallic NPs and the interference from the Cu 2p features. The areas of the Pt $4f_{7/2}$ peaks correspond roughly to about 2 mol % of the metal atoms detected within the depth sensitivity of XPS, accounting for most if not all of the Pt atoms in the catalyst. This suggests a placement of the Pt atoms on or near the surface region. Also to note is the identification of a partially oxidized Cu surface layer in the Cu 3p spectra (left) after the reaction. Because these spectra were acquired ex situ, it is in principle possible for the oxidation to take place during the handling of the samples. However, it should be noted that no oxidation was seen with the fresh samples (blue spectra), which were processed in a similar fashion.

a small peak can be clearly identified in all of the spectra at a binding energy (BE) of 70.7 ± 0.3 eV corresponding to the Pt $4f_{7/2}$ peak of metallic Pt (Figure 3, right panel). In fact, within the large experimental error due to the low Pt content of the samples and the overlapping Cu 2p peaks, it was determined that a large fraction, if not all, of the Pt atoms is within this $\sim 1-2$ nm surface shell probed by XPS (Supporting Information Table S1). 30,31

Surprisingly, infrared (IR) absorption spectroscopy studies using carbon monoxide as a probe molecule³² failed to identify Pt sites on the surface of our catalysts unless a quite high Pt content was added to the Cu NPs, $x \ge 0.2$, in the CuPt_x/SBA-15 samples (Figure 4). Recall that the optimum catalytic performance was obtained with much lower Pt fractions, $x \approx$ 0.001-0.01 (Figure 1). Here, the C-O stretching frequencies observed for the adsorbed CO are quite high (~2123 cm⁻¹) and can only be assigned to Cu-based, not Pt-based, surfaces.³³ We speculate that it may very well be that Pt does not fully segregate to the surface in these systems but rather stays in the subsurface region because the Cu surface becomes partially oxidized under the reaction conditions (in spite of the highly reducing environments used in these processes). The Cu 2p XPS data in Figure 3 (left panel) do show that a fraction of the detected Cu is in a nonmetallic state (Cu $2p_{3/2}$ BE = 933.8 \pm 0.2 eV) after the reaction (but not before; one single Cu $2p_{3/2}$ peak was seen for the fresh samples at BE = 932.6 ± 0.2 eV), and the values for the C-O stretching frequencies in Figure 4 are consistent with bonding to CuO_x rather than metallic Cu.³³ We speculate that, during catalysis, either the Pt atoms promote H2 activation from a

subsurface location or they are reversibly drawn to the surface upon exposure to the reaction mixture. Two more pieces of information are worth mentioning here: (1) Cu mobility and Pt segregation in Cu-Pt surfaces induced by exposure to CO have been seen before by a combination of techniques, including low-energy ion scattering (LEIS),³⁴ X-ray absorption spectroscopy (XAS),35 and in situ ambient-pressure XPS36 (although no similar effect was observed with H_2)³⁷ and (2) with CuPd_x alloys, no isotope exchange, indicative of molecular hydrogen activation, was detected with H₂ + D₂ mixtures unless Pd molar contents above approximately 15% were used. 38 These two observations, together with those resulting from our data, seem to indicate that hydrogen atmospheres may help with the diffusion of Pt (or Pd) atoms into the Cu subsurface and that CO may help with their segregation back to the surface. It should be noted that in our IR experiments CO was initially adsorbed at 125 K, too low of a temperature for the segregation of the Pt atoms to the surface to occur. Nevertheless, the catalysts in these experiments were then heated until the adsorbed CO desorbed from the surface, which happens around room temperature in all Cu-containing catalysts, and no new IR peaks indicating the segregation of CO to the surface were ever observed during this process. In the end, we conclude that although it may not be clear how exactly H₂ adsorbs and is activated in these so-called singleatom alloy catalysts under catalytic conditions, it must involve a process more complex than just coordinating and dissociating at individual Pt surface atoms.

We also investigated the behavior of the copper surfaces in terms of their ability to preferentially promote the hydrogenation of C=O bonds. First, the adsorption of unsaturated aldehydes (CTA, or but-2-enal - in this case, which is easier to handle in the IR cell thanks to its higher volatility compared to CMA) was probed using transmission infrared absorption spectroscopy. It was found that adsorption remains molecular on all of our CuPt_x/SBA-15 catalysts (for values of x of up to 0.1) even after annealing to 445 K; only the pure Pt catalyst showed signs of aldehyde decomposition and the production of adsorbed carbon monoxide (Supporting Information Figure S3). Furthermore, it was also evidenced that the peaks most affected by adsorption are those associated with the C=O bond, the multiple features around 1680 cm⁻¹, which all appear at higher values than that for CTA on pure SBA-15 (1668 cm⁻¹). In contrast, the C=C stretching mode peak seen at around 1640 cm⁻¹ is virtually unaffected by bonding to the bimetallic surfaces. All these suggest that the adsorption of unsaturated aldehydes on copper surfaces takes place through the C=O bond. Corroborating evidence comes from DFT calculations, which point to the most stable structure on Cu(111) at high coverages being a $\eta^1(O)$ -bonded adsorbate (Supporting Information Figure S4). Even at low coverages, the unsaturated aldehyde seems to prefer to bond to the Cu(111) surface in low coordination modes (Supporting Information Figure S4), in contrast with the high coordination preferred on Pt(111). Adsorption via a single bond between the oxygen atom and the copper surface at high coverages rather than the multiple coordination found on Pt may explain at least in part the selectivity for the catalytic hydrogenation of C=O bonds seen in Figure 1.

TPD experiments were also carried out with model Cu(110) single-crystal surfaces under UHV conditions to evaluate the intrinsic selectivity of copper as a catalyst for the hydrogenation of C=O versus C=C bonds. Two types of

CO/CuPt_x/SBA-15 IR Absorption Spectra vs. T_{anneal} CuPt_{0.00} CuPt_{0.00} CuPt_{0.05} 375 325 275 225 Femperature / K 175 CuPt_{0.2} CuPto. 325 225 175 1800 2000 1800 2000 1800 2000 1800 2000

Figure 4. IR absorption spectra for CO adsorbed on $\text{CuPt}_x/\text{SBA-15}$ catalysts of various compositions (x=0-1). Each panel corresponds to a different catalyst and shows the IR spectra as a function of temperature during heating, after initial adsorption at 125 K under 50 Torr CO. The main peak in all of the Cu-containing samples was seen at 2123 cm⁻¹, a value associated with the adsorption of CO on a CuO_x surface. Moreover, the desorption of all adsorbed species is complete after heating to room temperature, an indication of weak bonding to the surface. Only the pure Pt catalyst shows a main peak at a lower frequency (2088 cm⁻¹, shifting to 2063 cm⁻¹ at high temperatures) and stronger adsorption. Of particular significance is the fact that for CuPt_x compositions with $x \ge 0.1$, an additional peak is seen around 2045 cm⁻¹, possibly because of adsorption on multiple-atom ensemble surface sties involving Pt. However, even this adsorption is weak and displays a different C-O stretching frequency than CO bonded to isolated Pt surface atoms.

Wavenumber / cm⁻¹

experiments were performed with CMA coadsorbed with hydrogen: typical TPD runs, where the temperature of the surface is ramped in a linear fashion as mass spectrometry data are collected on the desorbing species, and isothermal (IsoTPD) tests, where the temperature is held constant and the data are collected versus time. Because molecular hydrogen adsorption on copper is activated, no reactivity was seen in these experiments with molecular H2 (the reason why Cu catalysts are in general inefficient at promoting hydrogenation reactions). Instead, hydrogen was dosed in atomic form, after gas-phase activation using a hot filament. Extensive studies were carried out by recording over 50 different masses in multiple TPD and IsoTPD experiments to help with the deconvolution and quantification of the data, which was carried out by using a procedure described in detail elsewhere;³⁹ representative results from these studies are shown in Figure 5. Oxygen-pretreated Cu(110) surfaces were used to better emulate the thin Cu oxide layer detected by XPS (Figure 3), but qualitatively similar results were obtained with clean Cu(110) as well (Supporting Information Figure S5). It is clear from these data that copper surfaces are almost 100% selective toward the primary formation of CMO; virtually no HCMA was detected in any of the experiments. It should be noted that only partial, albeit extensive, conversion was reached (21-24% of the unreacted CMA was detected, a likely consequence of the nature of these TPD setups) and that some fully-hydrogenated HCMO was detected in these cases as well (likely because CMO remains adsorbed on the surface long enough after been formed to be able to incorporate additional hydrogen atoms).

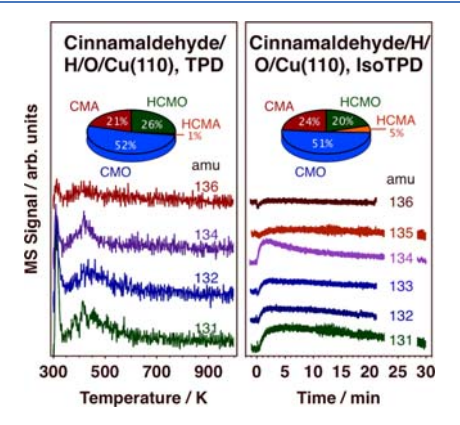


Figure 5. Regular (temperature-ramped, left panel) and isothermal (right) TPD results from hydrogenation experiments with CMA on oxygen-predosed (50 L, 500 K) Cu(110) single-crystal surfaces. For the regular TPD, the surface was saturated with atomic hydrogen, made via gas-phase activation of H₂ using a hot filament, prior to CMA adsorption, whereas in the IsoTPD experiments, time zero was set at the start of the exposure of the CMA-dosed O/Cu(110) surface to atomic H. In both types of experiments, it was determined that the primary product from the hydrogenation of CMA is CMO, which is made with almost 100% selectivity versus HCMA: the final yields are 51–52% for CMO and 1–5% for HCMA (the rest are unreacted CMA and fully hydrogenated HCMO, the latter suggesting that some of the initial products may remain on the surface after the initial H incorporation steps and undergo full hydrogenation).

An explanation for the selective behavior of Cu in these hydrogenation processes was explored further using DFT calculations. Figure 6 reports the potential energy surfaces

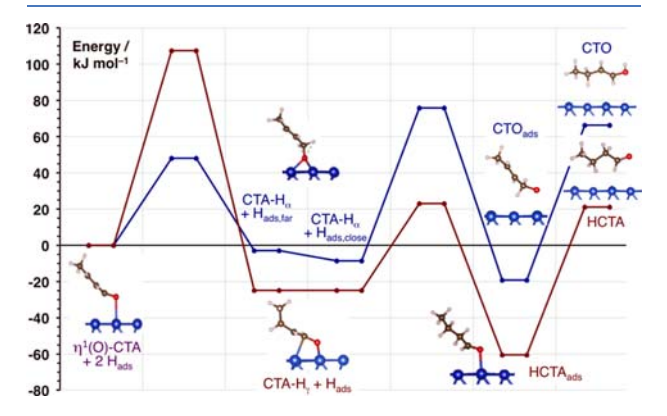


Figure 6. DFT calculations of the energetics of the optimized reaction coordinate for the conversion of CTA adsorbed on Cu(111) to either CTO (blue trace) or HCTA (red). A (2×2) periodic cell was used in all cases, corresponding to an initial aldehyde surface coverage of a quarter of a monolayer. It can be seen in this diagram that the rate-limiting step is the incorporation of the first hydrogen to CTA and that such a step displays a higher activation barrier toward the production of HCTA than for the formation of CTO. By contrast, the adsorbed HCTA was found to be more stable than the adsorbed CTO, suggesting that, in a competitive adsorption environment, the Cu surface may be primarily covered with HCTA.

calculated for the optimized pathways for CTA hydrogenation to either crotyl alcohol (CTO, or but-2-enol; blue trace) or dihydrocrotonaldehyde (HCTA, or butanal; red). Again, the simpler CTA instead of CMA was chosen for these studies to manage the cost of the calculations, but the trends seen are expected to be general for most unsaturated aldehydes. It appears that the defining rate-limiting step in these reactions is the incorporation of the first hydrogen atom into the adsorbed CTA. Quite possibly because of the fact that adsorption is through the oxygen atom, the barrier for the formation of the first intermediate on the way to the production of HCTA, via a H addition to the γ carbon of the aldehyde, is much higher $(E_{\rm act} = 108 \text{ kJ/mol})$ than that for the addition to the α carbon needed to eventually make CTO ($E_{act} = 48 \text{ kJ/mol}$). Consequently, the production of CTO is highly favored from a kinetic point of view on these Cu surfaces.

Finally, another observation worth highlighting from Figure 6 is that the relative energies of adsorbed HCTA ($E(HCTA_{ads})$ = -60 kJ/mol) and of adsorbed CTO ($E(\text{CTO}_{ads}) = -19 \text{ kJ/mol}$ mol) are lower than that of CTA (the reference state for these energy values, $E(CTA_{ads}) + 2 E_{ads}(H) = 0 kJ/mol)$. Moreover, the two products exhibit large adsorption energies $(E_{ads}(HCTA) = -82 \text{ kJ/mol}, E_{ads}(CTO) = -85 \text{ kJ/mol}).$ This means that in a competitive environment where the catalyst is exposed to mixtures of the saturated aldehyde, the unsaturated alcohol, and the unsaturated aldehyde, the Cu surface is expected to be covered mainly with the products, that is, with the first two molecules. Such a result is relevant to our discussion in that it was determined that the selectivity toward CMO production in our experiments, which were performed in a batch reactor (so the products accumulate in the reaction mixture over time), increases with increasing reaction time (Supporting Information Figure S6). This is accompanied by a rapid slowing down of the overall conversion rate, which is not due to catalyst poisoning, because such activity can be restored almost completely upon replacing the spent reaction mixture with a fresh one (Supporting Information Figure S6). It appears that, once made, a mixture of HCMA and CMO may saturate the surface and block sites for further catalysis. These adsorbates may also crowd the surface and with this increase the activation barrier for the first hydrogenation step to the CMA-H (or CTA-H $_\gamma$ in the calculations) surface intermediate that leads to HCMA (HCTA) production.

4. CONCLUSIONS

In conclusion, we show here that catalysts consisting of NPs made out of small amounts of Pt atoms diluted in Cu, dispersed on a silica support, are capable of selectively hydrogenating C=O bonds in the presence of C=C bonds in unsaturated aldehydes. This is, we believe, the first case where single-atom alloy catalysts have been tested for the control of selectivity between two parallel competing pathways. At first sight, the behavior seen in our experiments may be explained using a single-atom alloy model in which the high selectivity of copper surfaces for the incorporation of hydrogen atoms into the C=O unsaturated bonds of the adsorbed reactant is complemented with the ability of individual Pt atoms to perform the initial and required activation of molecular hydrogen. However, a few complications render this picture incomplete. For one, the surface of our dispersed CuPt_x catalysts seems to consist mainly of a thin oxidized Cu film, not metallic Cu, in spite of the fact that hydrogenation reactions are carried out under highly reducing environments. Moreover, the titration experiments using carbon monoxide as a probe failed to identify surface Pt atoms until reaching values of $x \approx 0.2$. This questions the accessibility of such atoms for H₂ activation during catalysis, unless the active site for this step consists of small ensembles of atoms that include Pt, possibly in the subsurface, or unless Pt segregates to the surface reversibly during the reaction. Finally, selectivity appears to be controlled at least in part by the preferential adsorption of the products (vs the reactant). This is a factor that, to the best of our knowledge, has not been considered previously.

It is also worth thinking about these single-atom alloy catalysts in the context of what is known about bimetallic catalysts in general. As mentioned earlier, much work has been published in recent years on the use of single-atom catalysis as a way to control selectivity in heterogeneous catalysis. 22-25 However, most of those catalysts consist of single metal atoms dispersed on an oxide or another type of covalent or inert support. Only in a few instances have single atoms of one type of metal (Pt) been diluted within NPs of a second metal (Cu), 28,29 as we report here. On the other hand, bimetallic catalysts have been used in industry extensively for many years. 40,41 Importantly, the prevalent picture used to describe the chemistry of such catalysts involves electron mixing and charge transfer across the constituent metals 42-44 to achieve somewhat of an average metallic behavior which can be described, to a first approximation, by the position of the center of the d band. In the new single-atom catalysis paradigm, the diluted metal atoms (Pt in our case) are basically treated as individual electronic entities instead. This helps explain the incorporation of the new catalytic functionality (H₂ activation) to the original monometallic (Cu) catalyst but is at odds with the prevailing description of alloys. The results reported here indicate that, indeed, although the single-atom

catalytic model appears to predict the new catalytic behavior, the explanation of how these catalysts operate is more nuanced than that implied by considering each metal separately. Other recent studies have alluded to the factors mentioned above, ^{36,45} but further in situ or operando surface characterization experiments will be required to get a clearer picture of the way these catalysts function.

ASSOCIATED CONTENT

S Supporting Information

The Supporting Information is available free of charge on the ACS Publications website at DOI: 10.1021/acscatal.9b02547.

Kinetic data for the hydrogenation of CMA with $\text{CuPt}_x/\text{SBA-15}$ catalysts as a function of NP composition and $P(H_2)$; estimated Pt content in our $\text{CuPt}_x/\text{SBA-15}$ catalysts; IR spectra of CTA adsorbed on the $\text{CuPt}_x/\text{SBA-15}$ catalysts; DFT calculations of the adsorbate structures and adsorption energies for CTA on Cu(111) and Pt(111) surfaces; TPD and IsoTPD for the hydrogenation of CMA with atomic hydrogen on clean Cu(110) single-crystal surfaces; and kinetic data from catalyst recycling experiments (PDF)

AUTHOR INFORMATION

Corresponding Author

*E-mail: zaera@ucr.edu.

ORCID ®

Yueqiang Cao: 0000-0002-1036-4049 Francisco Zaera: 0000-0002-0128-7221

Notes

The authors declare no competing financial interest.

ACKNOWLEDGMENTS

Financial support for this project was provided by a grant from the U. S. National Science Foundation, Division of Chemistry (NSF-CHE 1660433). YC acknowledges the 111 project of China (grant no. B08021, Ministry of Education of the People's Republic of China and State Administration of Foreign Experts Affairs of People's Republic of China) for traveling support for his visit to Riverside to perform the reported experiments. N.T. and J.G.S. thank DGAPA-UNAM project IN100516 and Conacyt grant A1-S-9070 for partial financial support. N.T. thanks DGAPA-UNAM for a sabbatical scholarship at the University of California, Riverside. Calculations were performed in the DGCTIC-UNAM Supercomputing Center, project LANCAD-UNAM-DGTIC-051.

REFERENCES

- (1) Blaser, H.-U. Heterogeneous catalysis for fine chemicals production. *Catal. Today* **2000**, *60*, 161–165.
- (2) Somorjai, G. A.; Park, J. Y. Molecular Factors of Catalytic Selectivity. *Angew. Chem., Int. Ed.* **2008**, *47*, 9212–9228.
- (3) Zaera, F. New Challenges in Heterogeneous Catalysis for the 21st Century. Catal. Lett. 2012, 142, 501-516.
- (4) Pang, S. H.; Medlin, J. W. Controlling Catalytic Selectivity via Adsorbate Orientation on the Surface: From Furfural Deoxygenation to Reactions of Epoxides. *J. Phys. Chem. Lett.* **2015**, *6*, 1348–1356.
- (5) Zaera, F. The Surface Chemistry of Metal-Based Hydrogenation Catalysis. ACS Catal. 2017, 7, 4947–4967.
- (6) Mäki-Arvela, P.; Hájek, J.; Salmi, T.; Murzin, D. Y. Chemoselective Hydrogenation of Carbonyl Compounds over Heterogeneous Catalysts. *Appl. Catal., A* **2005**, 292, 1–49.

(7) Medlin, J. W. Understanding and Controlling Reactivity of Unsaturated Oxygenates and Polyols on Metal Catalysts. *ACS Catal.* **2011**, *1*, 1284–1297.

- (8) Yuan, Y.; Yao, S.; Wang, M.; Lou, S.; Yan, N. Recent Progress in Chemoselective Hydrogenation of α,β -Unsaturated Aldehyde to Unsaturated Alcohol Over Nanomaterials. *Curr. Org. Chem.* **2013**, 17, 400–413.
- (9) Dong, Y.; Zaera, F. Selectivity in Hydrogenation Catalysis with Unsaturated Aldehydes: Parallel Versus Sequential Steps. *J. Phys. Chem. Lett.* **2018**, *9*, 1301–1306.
- (10) Gallezot, P.; Richard, D. Selective Hydrogenation of α,β -Unsaturated Aldehydes. *Catal. Rev.* **1998**, 40, 81–126.
- (11) Weng, Z.; Zaera, F. Sub-Monolayer Control of Mixed-Oxide Support Composition in Catalysts via Atomic Layer Deposition: Selective Hydrogenation of Cinnamaldehyde Promoted by (SiO₂-ALD)-Pt/Al₂O₃. ACS Catal. **2018**, *8*, 8513–8524.
- (12) Zhu, Y.; Zaera, F. Selectivity in the Catalytic Hydrogenation of Cinnamaldehyde Promoted by Pt/SiO₂ as a Function of Metal Nanoparticle Size. *Catal. Sci. Technol.* **2014**, *4*, 955–962.
- (13) Yao, Y.; Coyle, J. P.; Barry, S. T.; Zaera, F. Effect of the Nature of the Substrate on the Surface Chemistry of Atomic Layer Deposition Precursors. *J. Chem. Phys.* **2017**, *146*, 052806.
- (14) Yao, Y.; Guerrero-Sánchez, J.; Takeuchi, N.; Zaera, F. Coadsorption of Formic Acid and Hydrazine on Cu(110) Single-Crystal Surfaces. *J. Phys. Chem. C* **2019**, *123*, 7584–7593.
- (15) Kresse, G.; Furthmüller, J. Efficient iterative schemes forab initiototal-energy calculations using a plane-wave basis set. *Phys. Rev. B: Condens. Matter Mater. Phys.* **1996**, *54*, 11169–11186.
- (16) Blöchl, P. E. Projector Augmented-Wave Method. Phys. Rev. B: Condens. Matter Mater. Phys. 1994, 50, 17953–17979.
- (17) Perdew, J. P.; Burke, K.; Ernzerhof, M. Generalized Gradient Approximation Made Simple. *Phys. Rev. Lett.* **1996**, 77, 3865–3868.
- (18) Grimme, S.; Antony, J.; Ehrlich, S.; Krieg, H. A Consistent and Accurate Ab Initio Parametrization of Density Functional Dispersion Correction (DFT-D) for the 94 Elements H-Pu. *J. Chem. Phys.* **2010**, 132, 154104
- (19) Pham, T. T.; Lobban, L. L.; Resasco, D. E.; Mallinson, R. G. Hydrogenation and Hydrodeoxygenation of 2-Methyl-2-Pentenal on Supported Metal Catalysts. *J. Catal.* **2009**, *266*, 9–14.
- (20) Zheng, R.; Porosoff, M. D.; Weiner, J. L.; Lu, S.; Zhu, Y.; Chen, J. G. Controlling Hydrogenation of CO and CC Bonds in Cinnamaldehyde Using Silica Supported Co-Pt and Cu-Pt Bimetallic Catalysts. *Appl. Catal., A* **2012**, 419–420, 126–132.
- (21) O'Brien, C. P.; Miller, J. B.; Morreale, B. D.; Gellman, A. J. The Kinetics of H₂–D₂ Exchange over Pd, Cu, and PdCu Surfaces. *J. Phys. Chem. C* **2011**, *115*, 24221–24230.
- (22) Yang, X.-F.; Wang, A.; Qiao, B.; Li, J.; Liu, J.; Zhang, T. Single-Atom Catalysts: A New Frontier in Heterogeneous Catalysis. *Acc. Chem. Res.* **2013**, *46*, 1740–1748.
- (23) Gates, B. C.; Flytzani-Stephanopoulos, M.; Dixon, D. A.; Katz, A. Atomically Dispersed Supported Metal Catalysts: Perspectives and Suggestions for Future Research. *Catal. Sci. Technol.* **2017**, *7*, 4259–4275
- (24) Liu, J. Catalysis by Supported Single Metal Atoms. ACS Catal. 2017, 7, 34–59.
- (25) Wang, A.; Li, J.; Zhang, T. Heterogeneous Single-Atom Catalysis. *Nat. Rev. Chem.* **2018**, 2, 65–81.
- (26) Kyriakou, G.; Boucher, M. B.; Jewell, A. D.; Lewis, E. A.; Lawton, T. J.; Baber, A. E.; Tierney, H. L.; Flytzani-Stephanopoulos, M.; Sykes, E. C. H. Isolated Metal Atom Geometries as a Strategy for Selective Heterogeneous Hydrogenations. *Science* **2012**, 335, 1209–1212.
- (27) Lucci, F. R.; Liu, J.; Marcinkowski, M. D.; Yang, M.; Allard, L. F.; Flytzani-Stephanopoulos, M.; Sykes, E. C. H. Selective Hydrogenation of 1,3-Butadiene on Platinum—Copper Alloys at the Single-Atom Limit. *Nat. Commun.* **2015**, *6*, 8550.
- (28) Lucci, F. R.; Darby, M. T.; Mattera, M. F. G.; Ivimey, C. J.; Therrien, A. J.; Michaelides, A.; Stamatakis, M.; Sykes, E. C. H.

Controlling Hydrogen Activation, Spillover, and Desorption with Pd-Au Single-Atom Alloys. *J. Phys. Chem. Lett.* **2016**, *7*, 480–485.

- (29) Giannakakis, G.; Flytzani-Stephanopoulos, M.; Sykes, E. C. H. Single-Atom Alloys as a Reductionist Approach to the Rational Design of Heterogeneous Catalysts. *Acc. Chem. Res.* **2018**, 52, 237–247
- (30) Schurmans, M.; Luyten, J.; Creemers, C.; Declerck, R.; Waroquier, M. Surface Segregation in CuPt Alloys by Means of an Improved Modified Embedded Atom Method. *Phys. Rev. B: Condens. Matter Mater. Phys.* **2007**, *76*, 174208.
- (31) Yang, K.; Yang, B. Identification of the Active and Selective Sites over a Single Pt Atom-Alloyed Cu Catalyst for the Hydrogenation of 1,3-Butadiene: A Combined DFT and Microkinetic Modeling Study. *J. Phys. Chem. C* **2018**, *122*, 10883–10891.
- (32) Zaera, F. Infrared Absorption Spectroscopy of Adsorbed CO: New Applications in Nanocatalysis for an Old Approach. *ChemCatChem* **2012**, *4*, 1525–1533.
- (33) Xu, F.; Mudiyanselage, K.; Baber, A. E.; Soldemo, M.; Weissenrieder, J.; White, M. G.; Stacchiola, D. J. Redox-Mediated Reconstruction of Copper During Carbon Monoxide Oxidation. *J. Phys. Chem. C* **2014**, *118*, 15902–15909.
- (34) Andersson, K. J.; Calle-Vallejo, F.; Rossmeisl, J.; Chorkendorff, I. Adsorption-Driven Surface Segregation of the Less Reactive Alloy Component. *J. Am. Chem. Soc.* **2009**, *131*, 2404–2407.
- (35) Oxford, S. M.; Lee, P. L.; Chupas, P. J.; Chapman, K. W.; Kung, M. C.; Kung, H. H. Study of Supported PtCu and Pdau Bimetallic Nanoparticles Using In-Situ X-Ray Tools. *J. Phys. Chem. C* **2010**, *114*, 17085—17091.
- (36) Simonovis, J. P.; Hunt, A.; Palomino, R. M.; Senanayake, S. D.; Waluyo, I. Enhanced Stability of Pt-Cu Single-Atom Alloy Catalysts: In Situ Characterization of the Pt/Cu(111) Surface in an Ambient Pressure of CO. *J. Phys. Chem. C* **2018**, *122*, 4488–4495.
- (37) Simonovis, J. P.; Hunt, A.; Senanayake, S. D.; Waluyo, I. Subtle and Reversible Interactions of Ambient Pressure H₂ with Pt/Cu(111) Single-Atom Alloy Surfaces. *Surf. Sci.* **2019**, *679*, 207–213.
- (38) Gumuslu, G.; Kondratyuk, P.; Boes, J. R.; Morreale, B.; Miller, J. B.; Kitchin, J. R.; Gellman, A. J. Correlation of Electronic Structure with Catalytic Activity: H₂–D₂ Exchange across Cu_xPd_{1-X} Composition Space. ACS Catal. **2015**, 5, 3137–3147.
- (39) Wilson, J.; Guo, H.; Morales, R.; Podgornov, E.; Lee, I.; Zaera, F. Kinetic Measurements of Hydrocarbon Conversion Reactions on Model Metal Surfaces. *Phys. Chem. Chem. Phys.* **2007**, *9*, 3830–3852.
- (40) Sinfelt, J. H. Bimetallic Catalysts: Discoveries, Concepts and Applications; John Wiley and Sons: New York, 1983.
- (41) Yu, W.; Porosoff, M. D.; Chen, J. G. Review of Pt-Based Bimetallic Catalysis: From Model Surfaces to Supported Catalysts. *Chem. Rev.* **2012**, *112*, 5780–5817.
- (42) Rodriguez, J. A.; Goodman, D. W. The Nature of the Metal-Metal Bond in Bimetallic Surfaces. *Science* **1992**, *257*, 897–903.
- (43) Kitchin, J. R.; Nørskov, J. K.; Barteau, M. A.; Chen, J. G. Role of Strain and Ligand Effects in the Modification of the Electronic and Chemical Properties of Bimetallic Surfaces. *Phys. Rev. Lett.* **2004**, 93, 156801
- (44) Xin, H.; Vojvodic, A.; Voss, J.; Nørskov, J. K.; Abild-Pedersen, F. Effects of *D*-Band Shape on the Surface Reactivity of Transition-Metal Alloys. *Phys. Rev. B: Condens. Matter Mater. Phys.* **2014**, 89, 115114.
- (45) Darby, M. T.; Réocreux, R.; Sykes, E. C. H.; Michaelides, A.; Stamatakis, M. Elucidating the Stability and Reactivity of Surface Intermediates on Single-Atom Alloy Catalysts. *ACS Catal.* **2018**, *8*, 5038–5050.